An iron evaluation story: from TALYS model parameters to validation on the ASPIS benchmark with the Monte Carlo code TRIPOLI-4®

Valeria Raffuzzi[1*], Jean-Christophe Sublet[2], Cédric Jouanne[3], Arjan Koning[2], Dimitri Rochman[4]

[1]University of Cambridge, Trumpington Street, CB2 1PZ Cambridge, United Kingdom

[2]IAEA, NAPC-Nuclear Data Section, Wagramer Str. 5, 1220 Vienna, Austria

[3]Université Paris-Saclay, CEA, Service d'Etudes des Réacteurs et de Mathématiques Appliquées, 91191, Gif-sur-Yvette, France

[4]PSI, Forschungsstrasse 111, 5232 Villigen, Switzerland

*vr339@cam.ac.uk

doi.org/10.13182/PHYSOR22-37310

ABSTRACT

Iron is a widespread structural material in nuclear applications. However, some benchmark studies show that for many libraries, including TENDL-2019, producing good iron evaluations is still an open challenge. This work aims at improving TENDL-2019 ^{56}Fe and ^{54}Fe evaluations through feedbacks from experimental data and Monte Carlo results of the iron benchmark ASPIS. Part of the T6 code infrastructure was used to produce the evaluations. In the new evaluations, particular attention to resonance parameters and formalism was paid to address the importance of elastic scattering. The total inelastic scattering and inelastic continuum cross sections were shaped by modifying the input parameters of TALYS, one of the T6 codes. Additionally, it was necessary to normalise some reaction channels to those of JENDL-4.0. With the new files ASPIS results, obtained with the Monte Carlo code TRIPOLI-4®, improved noticeably compared to TENDL-2019. The evaluations and parameter setting modifications are to be included into TENDL-2021.

KEYWORDS: Nuclear Data, Iron Evaluation, TALYS, TENDL, ASPIS benchmark

1. INTRODUCTION

Iron is a widespread structural material and is regularly found in nuclear fission reactors, fusion devices and particle accelerators. Therefore, a correct set of nuclear data for the main iron isotopes is extremely important for nuclear application modeling. Generally, reactor criticality benchmarks are not particularly sensitive to iron. However, this is not the case for shielding benchmarks, where the deviation from experimental results is often noticeable for many libraries. This is widely acknowledged, and previous work has been undertaken to generate improved iron evaluations. For example, iron was included in the project CIELO, an international collaboration which focuses on producing new evaluations for important nuclides [1]. The main challenges were identified as generating reliable iron elastic and inelastic scattering cross sections and angular distributions. The difficulty is aggravated by the lack of reliable experimental data in some energy regions, as well as the existence of contradictory data.

Two benchmarks that highlight discrepancies between iron evaluations of different libraries are the SINBAD Winfrith Iron and Iron-88 Benchmark Experiments (ASPIS) [2][3]. They both consist of fission neutron transmission in a thick iron target with detectors at multiple depths. These benchmarks, especially

sensitive to ^{56}Fe and ^{54}Fe, show inaccuracies within most of the major libraries in use, with the partial exception of JENDL-4.0 [3][4]. For example, in the case of TENDL-2019, the calculated reaction rate is generally underestimated, and the discrepancy from experimental results reaches values as high as 40%.

This work was carried out in the framework of the code infrastructure T6, currently used to produce the library TENDL [5]. The goal is to use part of the T6 software, and in particular the nuclear reaction model code TALYS [6], to improve the iron evaluations of TENDL-2019. This paper focuses on the two main iron isotopes, ^{56}Fe and ^{54}Fe, whose natural isotopic abundance is respectively 91.8% and 5.8%. After the production of new evaluations, those were tested on the ASPIS Iron benchmark, simulated with the Monte Carlo code TRIPOLI-4® [7].

2. ASPIS IRON BENCHMARK

ASPIS Iron is a fission reactor physics benchmark used to verify the shielding properties of iron [8]. The neutron source is an enriched uranium slab, which releases fission neutrons into a thick iron target. Several detectors at multiple depths are placed into the iron, measuring reaction rates up to 120cm deep into the iron bulk. Different types of detectors were employed, due to their different energy thresholds. In particular, the reactions detected are ^{103}Rh(n,n'), ^{115}In(n,n') and ^{32}S(n,p), and their energy thresholds are respectively 50keV, 400keV and 1.5MeV. For more details on the benchmark geometry and material compositions please consult [2].

The approach chosen in this work to test the newly produced iron evaluations was to focus on the high energy detector first and progressively go down in energy. This approach is justified by the physics of shielding problems, since the source neutrons slow down in the material without generating further higher energy fission neutrons. The ^{32}S(n,p) detector, with an energy threshold of 1.5MeV, is extremely sensitive to the inelastic scattering continuum cross section, whose threshold is around 5MeV for both ^{56}Fe and ^{54}Fe. In that energy range, the continuum is the main contribution to the inelastic total cross section. Therefore, correct modeling the continuum and the inelastic cross section are of extreme interest in this paper. Next, actions in the resolved resonance range were necessary to achieve good accuracy.

3. CODE INFRASTRUCTURE

The goal of this work is to produce nuclear data evaluations for the main iron isotopes. This is done through some of the codes of the T6 infrastructure, described below.

3.1. T6, TALYS and Autotalys

The software T6 is used to generate the nuclear data libraries TENDL, whose goal is to maximise completeness, automatisation and reproducibility [5]. Here, a subsection of the T6 codes was used. In particular, the nuclear model code TALYS was run to generate central values of nuclear data in the keV - 30 MeV energy range [6]. TALYS uses several nuclear models to simulate reactions for disparate projectile particles. The default values of all model parameters for each projectile-target combination are hard-coded within TALYS. Therefore TALYS input files can contain multiplication factors for the model parameters, either with or without an energy dependence. During the production of TENDL, a so called TALYS 'best' input file is produced for each projectile-target combination through expert evaluation. This contains the best input parameters according to current knowledge. Additionally, TALYS can be run with a function called autonorm, which normalises the requested TALYS cross sections in a certain energy range to fit those from another library. After the normalisation, TALYS must be run a second time to adjust the remaining cross sections for consistency. For the resolved resonance range, TALYS can read resonance parameters from an input mf2 file, generally generated by the T6 code TARES [9], and reconstruct cross sections.

If uncertainty quantification and covariance matrices are desired, those can be obtained through the code TASMAN [10]. TASMAN, additionally, has the capability to run a linear sensitivity analysis on all the main

TALYS input parameters. This analysis provides a sensitivity matrix, composed of sensitivity coefficients which quantify all channel cross section variations given a TALYS parameter variation, for multiple ingoing energies. Finally, to produce a nuclear data evaluation file in ENDF-6 format with the outputs of TALYS and TASMAN, the code TEFAL [11] is needed.

Rather than executing each code independently, the whole flow can be run through the script autotalys. Autotalys allows several options: to include covariance calculation, to use autonorm, to use the 'best' TALYS input file, and several more. Also the TASMAN linear sensitivity analysis can be run through autotalys. Autotalys automatically creates the input files of the requested codes, and calls them in sequence to produce a complete evaluation. Some external codes are included as well, such as NJOY [12] and PREPRO [13], used to produce ACE files, PENDF files, and comparison plots between the newly produced TENDL evaluation and other libraries.

4. EVALUATION CONSTRUCTION

The first ^{56}Fe and ^{54}Fe evaluations were produced in an attempt to fit the inelastic cross section to experimental EXFOR data. Shaping cross sections can be achieved by modifying TALYS input parameters. An example of an extensive work where this is done automatically employing statistical methods can be found in [14]. In this work, the linear sensitivity analysis tool available in TASMAN was used to find the TALYS parameters that would impact the inelastic cross section without heavily modifying other channels. Both for ^{56}Fe and ^{54}Fe two optical model potential (OMP) parameters, *awdadjust* and *d1adjust*, were chosen. For any detail on the physics of the OMP consult the TALYS manual [6]. Fitting the inelastic scattering cross section to the experimental data was achieved in two separate ways, modifying each of the selected parameters individually. Those were added to the 'best' TALYS input file with a manually determined energy dependence. The results produced for ^{56}Fe are shown in Fig. 1. The white area in the plot highlights the energy range where the parameter modification took place. Out of two sets of EXFOR data shown in Fig. 1, the one with the most abundant recordings and lower uncertainties was followed. The two curves produced, each corresponding to the variation of one of the parameters, almost perfectly overlap. Out of the two, an evaluation with the modified *awdadjust* was produced, since it was shown to have less impact on the other channels' cross sections and angular distributions. However, the evaluation was tested with TRIPOLI-4® on the ASPIS benchmark, and the performance of the library degraded. As a consequence, a different approach, that included a comparison with integral experimental data rather than differential ones, was adopted.

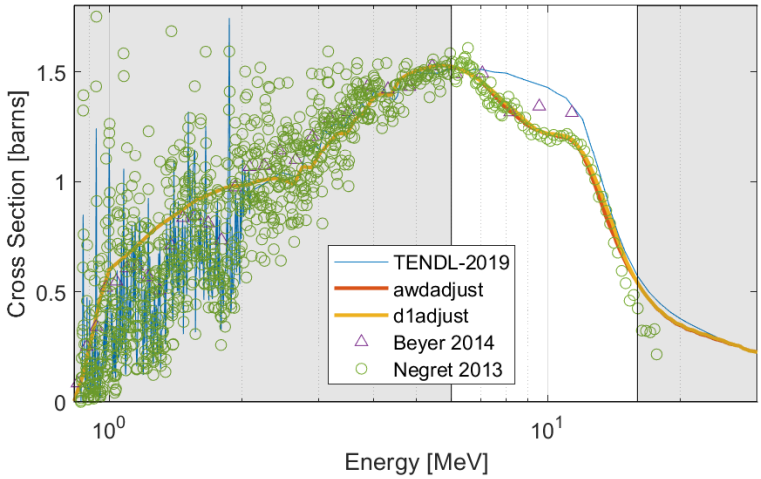

Figure 1: Inelastic scattering (MT4) cross section of ^{56}Fe. Experimental data from [15] and [16]

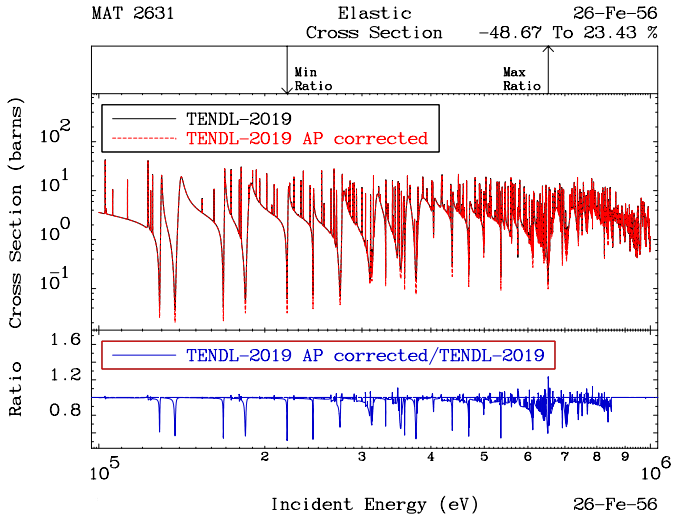

Figure 2: Effect of scattering radius (AP) on the elastic scattering cross section of ^{56}Fe

4.1. Fe-56 Evaluation

Nuclear data are usually optimised to reproduce experimental data as faithfully as possible. However, navigating experimental data can be challenging due to the presence of contradictory sets of data, missing uncertainties or missing data. In particular, differential experimental data are often not present for every reaction channel, and occasionally the existing data are unreliable due to experimental errors. Since the first evaluation attempt, based on fitting the inelastic cross section to experimental EXFOR data, was unsuccessful, a different approach was adopted. This relied on seeking important differences between a library that performs well on the ASPIS benchmark, i.e. JENDL-4.0, and TENDL-2019, and adjusting TENDL accordingly. At the same time, feedbacks from Monte Carlo ASPIS results were used to test and adjust the modifications implemented.

4.1.1. Scattering radius

In the resolved resonance range, which spans up to 850keV in JENDL-4.0 and TENDL-2019 for ^{56}Fe, the two libraries use identical resonance parameters. The only exception is one of the scattering radius (AP) values. More specifically, in TENDL-2019 the AP value for the momentum L=1 is equal to 0.5437 rather than JENDL-4's 0.4896. The parameters in use in JENDL-4.0 were determined by Froehner, Fabbri et al. for JEF-2. They are currently considered reference values, and can be found online on the NEA website. The scattering radius is used to define two important parameters, penetrability and hard-sphere phase shift [17], and has a very significant effect on, for example, the elastic cross section. The difference produced in the elastic cross section of TENDL-2019 by updating the scattering radius to the JEF-2 value can be seen in Fig. 2. This error was probably due to a typo or evaluator's distraction; therefore, it was corrected in this work.

4.1.2. TALYS parameters

Beyond the resolved resonance range, cross sections are computed by TALYS. As shown in Section 4, TALYS input parameters can be manipulated to shape cross sections. In this case, the process described at the beginning of Section 4 was adopted to modify the inelastic continuum. Since there are no EXFOR data

existing for the continuum, a few iterations were performed changing parameters and analysing ASPIS ^{32}S results, until they were satisfying. The final continuum can be seen in Fig. 3.

However, it must be noticed that modifying TALYS input parameters affects other channels too, as well as some angular distributions. Luckily, the impact on the angular distributions was considered minor. As for the modifications induced on the other cross sections, they were dealt with by using the TALYS function autonorm, as explained next.

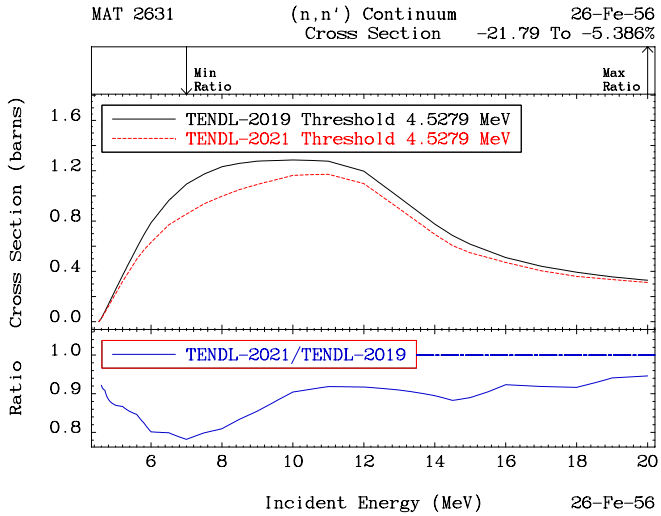

Figure 3: Comparison of ^{56}Fe inelastic continuum of TENDL-2019 and this work, i.e. TENDL-2021

4.1.3. Autonorm

The TENDL-2019 ^{56}Fe evaluation already makes use of a function called autonorm, described in Section 3.1. This function allows some requested reaction channels to be normalised to fit those from another library. The normalisation takes place beyond the resolved resonance energy range, i.e. in the TALYS energy domain. TENDL-2019 applies autonorm to the total inelastic (MT 4) and first 4 inelastic levels (MT 51-54) cross sections up to an energy of 14MeV. In the new evaluation, autonorm was used for the same channels up to 6MeV. The energy boundary was changed to avoid altering the continuum cross section, modified with the TALYS parameters. Additionally, it was previously mentioned that the use of input TALYS parameters different from the default ones impacted other cross sections too. In order to limit any possible drawback, also the elastic cross section was normalised to JENDL-4.0 from 850keV until 14MeV.

When using autonorm on ^{56}Fe, the oscillating - but not resonant - structure of MT 51 has to be reproduced faithfully. Therefore it is necessary to use a fine energy grid, including almost 400 energy points, rather than a coarser grid with 30 points, otherwise sufficient. Since a TALYS calculation has to be computed for each energy value, this function slows down the calculation significantly.

4.1.4. Background cross section

While carrying out the comparison between JENDL-4.0 and TENDL-2019, it was observed that JENDL-4.0 uses a background for the (n,γ) cross section between 500keV and 850keV. Since TENDL-2019 adopts the resolved resonance parameters from JENDL-4.0, sourced from JEF-2, also the background is included for consistency. Considering that this is a nonphysical modification, and that following the high energy modifications ASPIS results do not suffer from the lack of background, it was decided not to include it

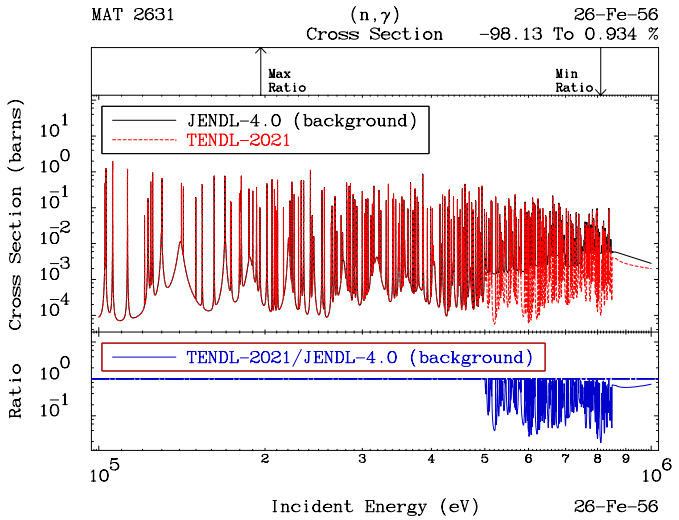

Figure 4: Comparison between ^{56}Fe capture cross section of JENDL-4.0, which employs a background, and this work, i.e. TENDL-2021

in the new evaluations. A comparison between the ^{56}Fe capture cross section of JENDL-4.0 and the one produced in this work is shown in Fig. 4.

4.2. Fe-54 Evaluation

Despite its natural abundance being less 6%, ^{54}Fe is extremely important within the ASPIS benchmark. In particular, in this work it was found to be responsible of approximately half of the TENDL-2019 reaction rate underestimation in ASPIS. The ^{54}Fe evaluation was built through an extremely similar process as ^{56}Fe, described below.

4.2.1. Resolved resonance parameters

By comparing TENDL-2019 to JENDL-4.0, it was noticed that the two libraries use a different resonance formalism. While the former adopts Multi-Level Breit Wigner (MLBW), the latter uses Reich-Moore (RM). Additionally JENDL-4.0 resonance parameters, taken from ENDF/B-VI.6, account for more resonances than TENDL-2019, whose parameters were obtained from the Atlas of Nuclear Resonances [18]. Once again, the different formalism and parameters produce a noticeable difference in the resolved resonance range, for example in the elastic cross section, as shown in Fig. 5. Therefore, Reich-Moore was adopted in this work, as well as the same resonance parameters of JENDL-4.0.

4.2.2. Autonorm

To make sure that the inelastic cross section was modeled correctly, autonorm was used once again. Like in the case of ^{56}Fe, autonorm was used on the total inelastic cross section and on some inelastic levels. MT 51-53 and MT 55 were selected as the first inelastic levels with a significantly high cross section, and normalised to JENDL-4.0. The normalisation was carried out until 6MeV. At the same time, the elastic cross section was normalised up to 14MeV. This was done to allow changing TALYS parameters to shift the continuum. However, it was noticed that after using autonorm, the continuum was renormalised by the second TALYS run. The new inelastic and continuum cross sections, shown in Fig. 6, were considered

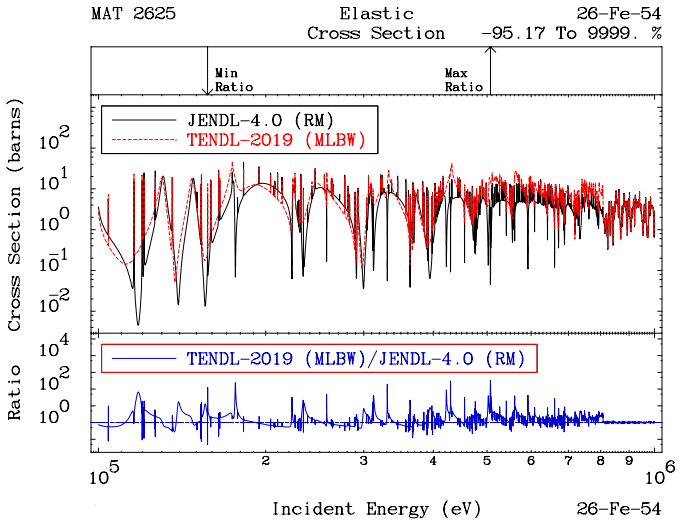

Figure 5: Different resonance formalism and parameters between JENDL-4.0, using RM, and TENDL-2019, using MLBW, on the elastic scattering cross section of ^{54}Fe

satisfying, so no further work was performed on them. This outcome is optimal since no angular distribution modification was induced by changing TALYS input parameters.

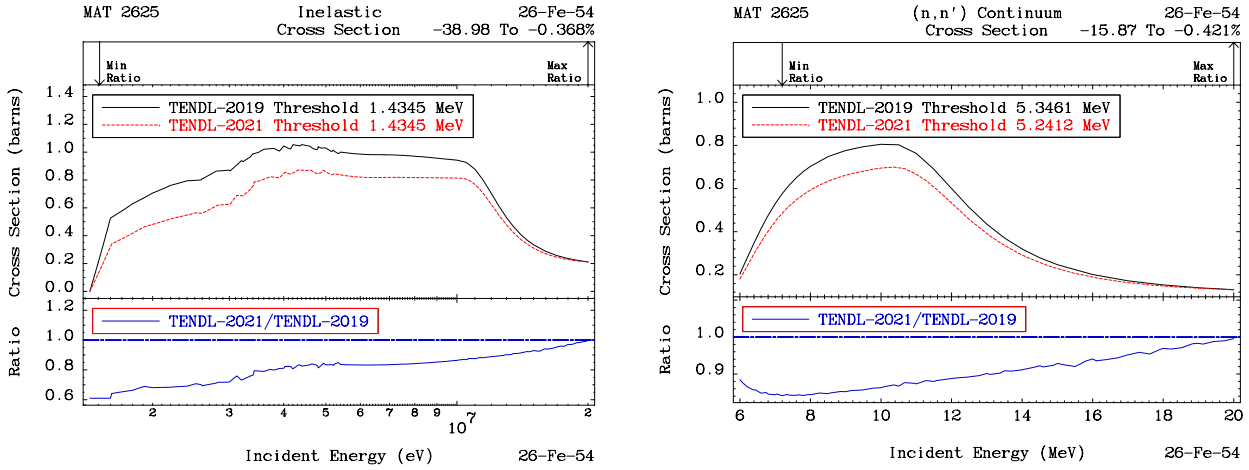

Figure 6: ^{54}Fe inelastic cross section (left) and continuum (right) of TENDL-2019 and this work, i.e. TENDL-2021

4.2.3. Background cross section

Analogously to ^{56}Fe, also in the case of ^{54}Fe a background cross section is included in JENDL-4.0. However, this was deemed unnecessary in the new evaluation, which only relies on resonance parameters to construct the capture cross section up to approximately 800keV. The comparison between the two (n,γ) cross sections is presented in Fig. 7.

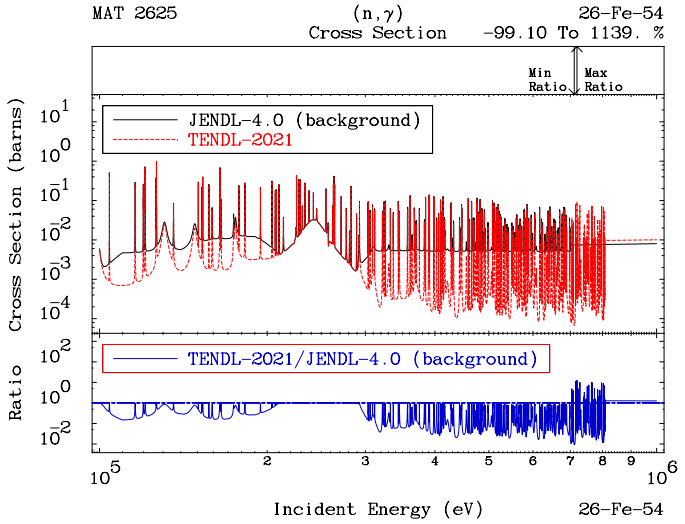

Figure 7: Comparison between ^{54}Fe capture cross section of JENDL-4.0, which employs a background, and this work, i.e. TENDL-2021

5. ASPIS IRON MONTE CARLO RESULTS

The two evaluations produced with part of the T6 software, run by autotalys, have been tested on the ASPIS Iron benchmark. To do so, they were used in combination with the rest of the TENDL-2019 library. The final results, compared with TENDL-2019 as well as other libraries, are presented in Fig. 8. The plots show the ratio between calculated and measured reaction rates (C/E). The new evaluations improved upon TENDL-2019 results for all detectors. The results are broadly within experimental uncertainties, except for the ^{103}Rh detector, where the reaction rate is slightly underestimated. However, the decreasing trend produced by TENDL-2019 for all detectors has been eliminated.

Also the individual effect of each modification with respect to TENDL-2019 on APSIS was analysed, but results cannot be reported for the sake of brevity. A brief summary is included. As expected, resonance parameters have a huge impact on the two low energy detectors, while they do not impact the high energy one at all. Normalising the first inelastic scattering levels to the ones of JENDL-4.0 also improved the low energy detectors, while normalising the elastic cross section brought a strong contribution in all energy ranges. The continuum was proven to be extremely important for the high energy detector, while not affecting the low energy ones. The contributions of the two new files, ^{56}Fe and ^{54}Fe, had an approximately equivalent impact on the final result, compared to the results produced using entirely TENDL-2019 files.

6. SUMMARY AND CONCLUSIONS

This paper summarises the production process of new evaluation files for ^{56}Fe and ^{54}Fe with the T6 infrastructure, used to produce the TENDL's libraries since 2008. Afterwards, the new files were tested by simulating the shielding benchmark ASPIS Iron with the Monte Carlo code TRIPOLI-4®.

An initial evaluation attempt, based on fitting the inelastic scattering cross section to differential experimental data, was performed. However, the evaluation produced did not improve the Monte Carlo results on the ASPIS benchmark. It must be noted that scattering cross sections are challenging to measure, thus existing experimental data might be questionable in some cases. Therefore, it was concluded that different modifications were necessary for both ^{56}Fe and ^{54}Fe. These included actions such as modifying some resonance parameters, normalising relevant reaction channels to JENDL-4.0, which performs well on ASPIS,

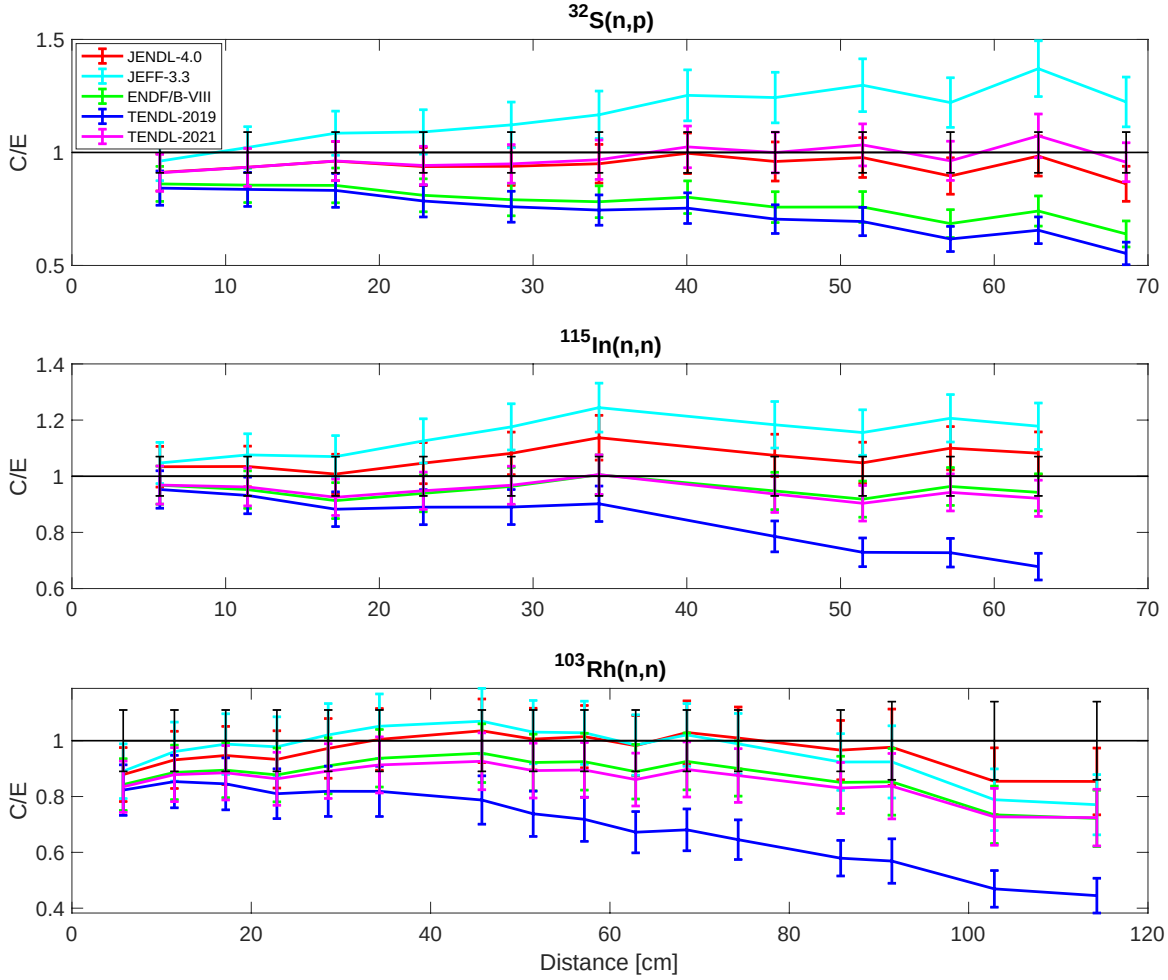

Figure 8: ASPIS benchmark results of different libraries for three detector types

and occasionally varying some TALYS input parameters to shape the inelastic continuum cross section. At the same time, it was observed that the use of a background in the resolved resonance range of the capture and total cross section, present in JENDL-4.0 for both ^{56}Fe and ^{54}Fe, was not necessary within this work. This is seen as an advantage, since the introduction of a background has negative side effects when self-shielding and temperature need to be taken into account.

The new evaluations showed significant improvements compared to TENDL-2019. However, future work could be done to address, for example, the ^{57}Fe evaluation as well. Additionally, further benchmarks should be run to test if the new evaluations perform well in different physical settings and energy ranges. The ASPIS benchmark could also be run using MCNP, which takes ACE files as an input rather than PENDF files, to corroborate the results produced by TRIPOLI-4®.

After the successful testing of the new evaluations on the SINBAD benchmark ASPIS Iron, the new parametric settings have been included into the TENDL production pipeline.

ACKNOWLEDGEMENTS

TRIPOLI-4® is a registered trademark of CEA. The authors thank EDF for partial financial support.

REFERENCES

[1] M. Herman, A. Trkov, R. Capote, G. P. Nobre, D. A. Brown, R. Arcilla, et al. "Evaluation of Neutron Reactions on Iron Isotopes for CIELO and ENDF/B-VIII.0." *Nuclear Data Sheets*, **volume 148**, pp. 214–253 (2018). URL https://doi.org/10.1016/j.nds.2018.02.004.

[2] J. Butler, M. D. Carter, A. McCracken, and A. Packwood. "Results and Calculational Model of the Winfrith Iron Benchmark Experiment." Technical report, NEACRP-A-629 (1984).

[3] B. Kos and I. A. Kodeli. "MCNP modelling of the ASPIS Iron88 SINBAD shielding benchmark." Technical report, INDC International Nuclear Data Committee (2018).

[4] C. Jouanne. "Sensitivity of the shielding benchmarks on variance-covariance data for scattering angular distributions." *Nuclear Data Sheets*, **volume 118**(1), pp. 384–387 (2014). URL http://dx.doi.org/10.1016/j.nds.2014.04.087.

[5] A. J. Koning, D. Rochman, J. C. Sublet, N. Dzysiuk, M. Fleming, and S. van der Marck. "TENDL: Complete Nuclear Data Library for Innovative Nuclear Science and Technology." *Nuclear Data Sheets*, **volume 155**, pp. 1–55 (2019). URL https://doi.org/10.1016/j.nds.2019.01.002.

[6] A. Koning, S. Hilaire, and S. Goriely. "Talys-2.0: Simulation of nuclear reactions." Technical report, NDS.IAEA.ORG (2020).

[7] E. Brun, F. Damian, C. M. Diop, E. Dumonteil, F. X. Hugot, C. Jouanne, et al. "Tripoli-4®, CEA, EDF and AREVA reference Monte Carlo code." *Annals of Nuclear Energy*, **volume 82**, pp. 151–160 (2015). URL http://dx.doi.org/10.1016/j.anucene.2014.07.053.

[8] M. Carter, M. Chestnutt, and A. McCracken. *The ASPIS iron benchmark experiment - results and calculational model* (1981).

[9] D. Rochman. "TARES-1.3: Generation of resonance data and uncertainties." Technical report, NRG PSI-XX (2017).

[10] A. Koning. "TASMAN-2.0 - Statistical software for TALYS: Uncertainties, sensitivities and optimization." Technical report, NDS.IAEA.ORG (2021).

[11] A. Koning. "Tefal-2.0: Making ENDF-6 nuclear data libraries from TALYS." Technical report, NDS.IAEA.ORG (2021).

[12] R. Macfarlane, D. W. Muir, R. M. Boicourt, A. C. I. Kahler, and J. L. Conlin. "The NJOY Nuclear Data Processing System, Version 2016." Technical report, LA-UR-17-20093 (2017). URL https://permalink.lanl.gov/object/tr?what=info:lanl-repo/lareport/LA-UR-17-20093.

[13] D. E. Cullen. "PREPRO 2021: 2021 ENDF/B Pre-processing Codes." Technical report, IAEA-NDS-0238 (2021).

[14] G. Schnabel, H. Sjöstrand, J. Hansson, D. Rochman, A. Koning, and R. Capote. "Conception and Software Implementation of a Nuclear Data Evaluation Pipeline." *Nuclear Data Sheets*, **volume 173**, pp. 239–284 (2021).

[15] R. Beyer, R. Schwengner, R. Hannaske, A. R. Junghans, R. Massarczyk, M. Anders, et al. "Inelastic scattering of fast neutrons from excited states in 56Fe." *Nuclear Physics A*, **volume 927**, pp. 41–52 (2014). URL http://dx.doi.org/10.1016/j.nuclphysa.2014.03.010.

[16] A. Negret, C. Borcea, P. Dessagne, M. Kerveno, A. Olacel, A. J. Plompen, et al. "Cross-section measurements for the Fe 56 (n, xnγ) reactions." *Physical Review C - Nuclear Physics*, **volume 90**(3), pp. 1–15 (2014).

[17] A. Trkov and D. Brown. "ENDF-6 Formats Manual: Data Formats and Procedures for the Evaluated Nuclear Data Files." Technical report, Brookhaven National Laboratory (2018).

[18] S. F. Mughabghab. *Atlas of Neutron Resonances*, volume 1 and 2. Elsevier, 6 edition (2018).